Quasi-two-dimensional plasmons of a single δ-doped layer in GaAs studied by high-resolution electron-energy-loss spectroscopy

C. Lohe, A. Leuther, A. Förster, and H. Lüth
Institut für Schicht- und Ionentechnik, Forschungszentrum Jülich (KFA), Postfach 1913, D-5170 Jülich, Germany
(Received 18 May 1992; revised manuscript received 7 October 1992)

High-resolution electron-energy-loss spectroscopy (HREELS) is used to study δ-doped GaAs samples with varying silicon dopant concentration. The δ-doped layers were grown by molecular-beam epitaxy at a substrate temperature of 600 °C and the silicon atoms were incorporated 20 nm underneath the surface. Characteristic loss structures are observed in the HREEL spectra and are attributed to the excitation of quasi-two-dimensional (2D) plasmon modes confined to the δ-doped region. A three-layer model of a confined free-electron gas is presented to understand the nature of the quasi-2D plasmon loss features. The experimental loss spectra are compared with simulations calculated self-consistently for free-electron density profiles in δ-doped GaAs. The spread of the dopant atoms and the level of electrically active dopants are fitting parameters. A significant difference is observed between profiles resulting from doping concentrations in the 10^{12} cm^{-2} and in the 10^{13} cm^{-2} range. In the samples with low doping levels all silicon atoms are incorporated as electrically active centers and the dopants segregate asymmetrically in direction of growth. In the samples with high doping levels autocompensation and an additional Si-pair diffusion process appear where the dopant diffuses symmetrically around its original location.

I. INTRODUCTION

Recently there has been considerable interest in locally restricted, so called δ doping of GaAs and $Al_xGa_{1-x}As$ layer systems.[1] This δ-doping technique plays an important role in the fabrication of modulation-doped $GaAs/Al_xGa_{1-x}As$ heterostructures with both very high electron mobilities and densities and in quantum-electronic and photonic device research[1]. For n-type doping the growth is interrupted to deposit Si donors on the surface. Subsequent growth is assumed to bury these donors. If the Si donors are confined in a few monolayers, the doping profile becomes narrower than the spatial extent of the electron wave functions. Therefore one expects to observe effects of a two-dimensional (2D) electron gas.[2–5]

However, in the recent years, several investigations by means of magnetotransport measurements,[2–5] secondary-ion mass spectrometry (SIMS),[6–10] capacitance-voltage (CV) profile measurements,[11–13] and Raman spectroscopy[14] have shown that the ideal δ-function-like doping profile is not realized in practice. The Si donors spread over several tens of monolayers mostly in the direction of growth.[4,6,15,16]

Although the Si donors are not confined in just two or three layers, they generate a V-shaped potential well in GaAs with a quasi-2D electron gas. The electron energies for motion perpendicular to the surface are quantized into 2D subbands.[2–5] The total depth of the well depends sensitively on the spreading of the donors. The level structure and the expected subband occupations change only slowly.[3]

In this paper high-resolution electron-energy-loss spectroscopy (HREELS) is used to investigate δ-doped GaAs layers. When using collective surface excitations as probes, the information depth of HREELS — unlike other electron surface techniques — can easily be tuned over a wide spatial range by changing the kinetic energy and the angle of incidence of the probing electrons in the experiment. Our main interest is the correlation of plasmon loss features in the HREEL spectra attributed to the quasi-2D electron gas in the δ-doping layer, and the dopant profile, e.g., the spreading of the Si donors during growth. Numerical calculations have been used to fit the HREELS data to a simple model with a step-function-like doping profile. We show that the observed loss features are caused by plasmon modes in the quasi-2D electron gas of the δ-doping layer. Analytic calculations of the effective dielectric function of a simple three-layer system are made to derive the dispersion relation of the associated plasmon modes.

II. EXPERIMENT

GaAs structures with a Si δ-doped layer were grown in a Varian Mod Gen II molecular-beam-epitaxy (MBE) system. Each structure was grown on a GaAs(100) substrate and consists of an undoped 0.5-μm-thick GaAs buffer layer (background doping $p \leq 10^{14}$ cm^{-3}) and a single δ layer close to the surface. The δ-doping concentrations N_{Si} are 0.64 and 2.6×10^{13} cm^{-2} Si atoms

deposited 20 nm beneath the surface. The GaAs growth was interrupted during the evaporation of Si. The growth rate for GaAs was 0.8 μm/h and the substrate temperature during growth was 600 °C, as determined by an Ircon infrared pyrometer. The growth process was terminated by cooling down the wafer to −10 °C within the arsenic beam. This procedure provides an arsenic passivation layer on the GaAs surface, which is required for subsequent handling in atmosphere.

5 mm ×10 mm samples were cleaved from the wafers and mounted on a sample holder. The holder was equipped with a 25-μm-thin sawtooth folded tantalum heating foil on the back side of the sample. The loaded sample holder was inserted into a turbomolecular pumped UHV system (base pressure 1×10^{-6} Pa) and the sample was heated by a current through the tantalum foil to about 150 °C and held at this temperature for 15 h in order to remove gaseous contaminations.

Next, the sample and holder were transferred to the HREELS analysis chamber by means of a magnetic transfer system. This analysis chamber is pumped by an ion getter pump and a titanium sublimation pump (base pressure below 5×10^{-9} Pa). It is equipped with a HREEL spectrometer (our design), a low-energy electron diffraction (LEED) system, and an Auger electron spectrometer (AES). While the arsenic passivation layer was removed by heating the sample to 400 °C for about 10 min, the system pressure increased to about 1×10^{-6} Pa. The sample temperature during decapping was measured by an Ircon infrared pyrometer. The end of the decap process was indicated by a decrease of the system pressure and a slight variation in the color of the sample surface.

After desorption of the arsenic passivation layer surface contaminations were checked by AES and HREELS. For both techniques any contamination was below the detection limit. LEED showed clear 1×1 spots with a light 4×4 superstructure, indicating an As-rich (100) surface.

HREEL spectra were aquired in specular geometry with primary electron energy E_0 varying between 2 and 23 eV and an incident angle θ between 50° and 75° to the surface normal. The full width at half maximum (FWHM) of the directly transmitted beam through the spectrometer is 7 meV. Samples which had been grown on an undoped substrate were prepared for measurement of the Hall mobility and the 2D free-electron density of the δ doping at room temperature.

III. RESULTS

In HREEL spectra of a semi-insulating GaAs sample without doping (not shown here) only loss features attributed to (multiple) excitations of the surface mode of the GaAs optical phonon at (multiple of) 36 meV appear. There, the width of the quasielastic peak at half maximum is 9 meV, close to the resolution of the HREEL spectrometer. When there is a Si δ-doping level, $N_{Si} = 6.4 \times 10^{12}$ cm^{-2}, 20 nm beneath the surface (sample Nos. MBE 2182 and 3087), the HREEL spectra change significantly, as shown in Fig. 1. The width of the quasielastic peak is increased up to a FWHM of 75 meV

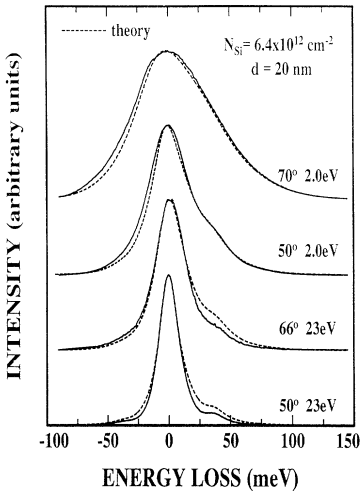

FIG. 1. HREEL spectra of a δ-doped GaAs structure with 6.4×10^{12} cm^{-2} silicon atoms 20 nm beneath the surface (solid lines). Theoretically simulated spectra in dashed line are obtained from a simple doping profile model [see Fig. 4(a)]. The broadening in the spectra is caused by excitations of a plasmon mode in the quasi-2D electron gas of the δ layer.

for a primary energy $E_0 = 2$ eV and an angle of incidence $\theta = 70°$. The GaAs optical surface phonon is completely obscured by a broad loss continuum. The integrated intensity of this loss continuum normalized to the intensity of the quasielastic peak is plotted in Fig. 2 as a function of the kinematic factor $1/k_0 \cos\theta$, where k_0 is the wave vector of the incident electrons with a kinetic energy of E_0. Two identically grown δ-doped GaAs wafers (MBE 2182 and 3087) were used to obtain the data. There is a linear correlation between the integrated intensity and the kinematic factor.

HREEL spectra from two different samples with the δ-doping level $N_{Si} = 2.6 \times 10^{13}$ cm^{-2} (MBE 2205 and 3123) and recorded under differing experimental conditions (E_0 and θ) are shown in Fig. 3. The strong energetic broadening of the quasielastic peak as in the spectra

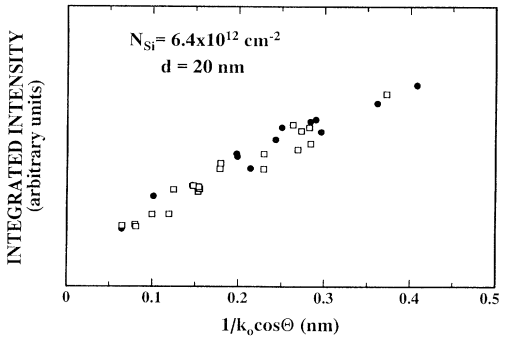

FIG. 2. Integrated intensity of the whole HREEL spectra divided by the intensity of the quasielastic peak vs kinematical factor of the probing electrons. Open squares (MBE 2182) and closed circles (MBE 3087) indicate two different wafers each with 6.4×10^{12} cm^{-2} silicon atoms 20 nm beneath the surface.

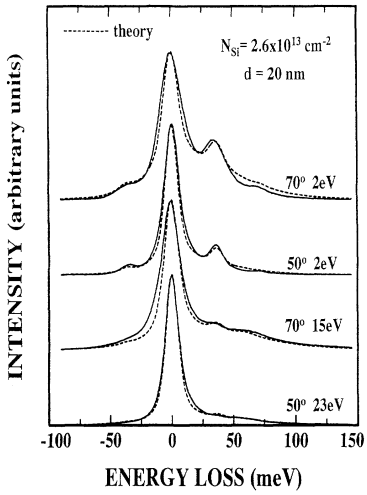

FIG. 2. Integrated intensity of the whole HREEL spectra divided by the intensity of the quasielastic peak vs kinematical factor of the probing electrons. Open squares (MBE 2182) and closed circles (MBE 3087) indicate two different wafers each with 6.4 $\times 10^{12}$ cm^{-2} silicon atoms 20 nm beneath the surface.

of Fig. 1 is not observed. However, we observe a slight broadening compared to GaAs without any doping. A new broad loss feature arises at about 60 meV for high primary beam energies (compare Fig. 6).

Additionally, Hall measurements were made on both δ-doped structures. The Hall free-electron density N_{Hall} and the Hall mobility μ_{Hall} at room temperature are listed in Table I.

The surface potential was used as a surface sensitive quantity to characterize the status of the GaAs surface after decapping. Therefore, in a separate UHV system equipped with an ultraviolet photoemission spectrometer (UPS) measurements of the band bending at the GaAs surface were performed. The decapping process of the arsenic passivation layer was identical to that in the HREELS system. We derived a surface potential, i.e., a difference of 0.65 eV between the conduction-band edge E_C and the Fermi level E_F at the surface. This value is in agreement with the data known from literature.[17]

IV. DISCUSSION

For modeling our experimental results we first consider a realistic spreading of the dopants in a δ-doped layer. The spatial spreading of the electrically active donors and the resulting volume doping density vary with the temperature of the substrate during growth.[6,7,9,15,18] There is a saturation of the volume doping density, closely corresponding to the solubility limit for the given temperatures.[4,14] Below a δ-doping level of about $N_{\mathrm{Si}} < 1.2 \times 10^{13}$ cm^{-2}, all silicon atoms are expected to be electrically active.[4,10,12] With higher doping levels compensation effects occur[12,19] and DX centers become relevant.[19]

In order to fit our HREEL spectra we have to model the spatial distribution of the dopant in our samples. Thereby we distinguish two different processes for the rearrangement of the Si donors during growth. For the first process we assume that the Si donors only spread asymmetrically in the direction of growth.[4,6,15,16] This process is a Fermi-level pinning-induced segregation during growth, caused by the space-charge field which drives the positively charged donors towards the surface.[20] The second process is considered to be a symmetrical diffusion of the donors with respect to their original location. In our model the doping profiles according to these processes are both roughly simplified by rectangular-shaped functions. The doping model is then used as an input for a numerical simulation of HREEL spectra. Based on the assumed dopant distribution a self-consistent calculation of the conduction-band profile is performed in which the Schrödinger and Poisson equations are solved. The obtained free-electron density profile $n(z)$ is then used for the calculation of the dielectric scattering cross section in HREELS. See Appendix A for details.

In the case of the low δ-doping level, $N_{\mathrm{Si}} = 6.4 \times 10^{12}$ cm^{-2}, the segregation process towards the surface dominates and we suppose all Si atoms to be electrically active. Here we use the spatial spreading length of the donors in the growth direction as a fitting parameter to our HREELS data, while the product of spreading length and volume doping level is kept constant at 6.4×10^{12} cm^{-2}. The model of the doping profile of the low-doped δ structure is shown in Fig. 4(a).

Although the δ layers are doped with an electrically active dopant concentration N_D, the number of free electrons N_E is considerably lower than N_D due to band bending at the GaAs surface. Some of the free electrons supplied by the donors are localized in surface states and form a barrier. The resulting conduction-band profile and the associated free-electron density profile $n(z)$ for a doping level $N_{\mathrm{Si}} = 6.4 \times 10^{12}$ cm^{-2} are shown in Fig. 5. The integrated area of this profile yields the total number of free electrons N_E in the δ layer. These calcula-

TABLE I. Experimental doping concentration N_{Si} and depth d of the Si δ-doped GaAs structures. Free-electron concentration N_{Hall} and mobility μ_{Hall} obtained from Hall measurements. Electrically active doping concentration N_D and free-electron concentration N_E obtained from a simulation of the HREEL spectra (see Appendix A) using a simple doping profile model (Fig. 4).

N_{Si} (cm^{-2})	d (nm)	N_{Hall},300 K (cm^{-2})	μ_{Hall},300 K (cm^2/V s)	N_D (cm^{-2})	N_E (cm^{-2})
6.4 $\times 10^{12}$	20	9.5 $\times 10^{11}$	1550	6.4 $\times 10^{12}$	1.3 $\times 10^{12}$
2.6 $\times 10^{13}$	20	9.3 $\times 10^{12}$	865	1.9 $\times 10^{13}$	9.5 $\times 10^{12}$

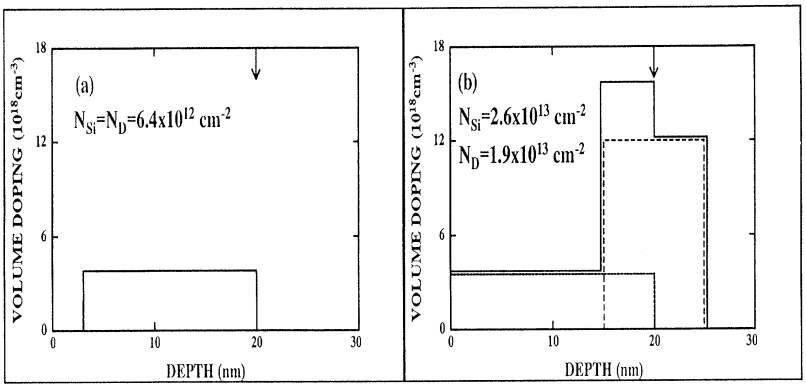

FIG. 4. Doping profile models of the δ-doped GaAs structures. The spreading of the dopants is simplified by rectangles (solid and dashed lines). For the low-doped structure (a) there is only an asymmetric spreading towards the direction of growth. In addition, a symmetric diffusion of the dopant arround its intentional location is considered for the high-doped structure (b). In that case not all the silicon atoms are electrically active. The resulting doping profile is shown as a solid line. The arrow indicates the original location of the δ-doping during growth.

tions have been made for a variety of different spreading lengths in our doping model.

The best fits for the low-doped δ structure together with the experimental spectra are shown in Fig. 1. There is good agreement with our experimental data. The broad energy-loss continuum leading to a broadening of the quasielastic peak is well reproduced by our model. A spreading of 17 nm of the Si donors towards the GaAs surface has been used to fit the HREEL spectra. This value is in agreement with the spreading length measured by Wagner *et al.*[14] and Santos *et al.*[15] with a similar doping level and a similar substrate temperature during growth. The volume doping density of the δ layer in our model is $3.8 \times 10^{18}\,\mathrm{cm}^{-3}$.

For the high δ-doping level $N_{\mathrm{Si}} = 2.6 \times 10^{13}\,\mathrm{cm}^{-2}$ we have to consider both processes of rearrangement of the Si donors, the asymmetrical segregation to the surface, and a symmetrical diffusion with respect to the original δ-doping location. The spreading length towards the surface is assumed to be identical to the thickness of the GaAs top layer (20 nm). Here the spreading length of the symmetrical diffusion process is used as a free parameter to fit the experimental data. In addition, the volume doping levels for both processes are used as parameters to fit the HREEL spectra of the high-doped δ structure. The sum of the electrically active dopants N_D is lower than the concentration of built-in Si atoms N_{Si} because compensation becomes relevant. The resulting doping model of the high-doped δ structure is shown in Fig. 4(b).

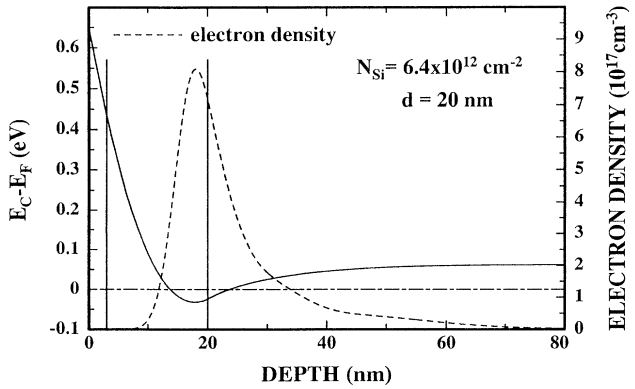

FIG. 5. Self-consistently calculated potential profile (conduction-band edge, solid line) and free-electron density profile (dashed line) for the doping profile model of Fig. 4(a). The perpendicular lines indicate the spreading range of the dopants.

The HREELS simulations have been performed as for the low-doped δ structure (see Appendix A). The best fits yield a segregation of $7\times10^{12}\,\mathrm{cm}^{-2}$ Si donors to the direction of the surface. In addition, $1.2\times10^{13}\,\mathrm{cm}^{-2}$ Si donors diffuse symmetrically over a range of 10 nm [Fig. 4(b)]. The corresponding electrically active dopant concentration N_D and the calculated free-electron density N_E in the δ layers together with the values obtained by Hall measurements are compared in Table I. The volume density of the donors segregating into growth direction is very similar to that obtained with the low-doped sample. An estimation of the coefficient according to the symmetric diffusion yields $D = 2.8 \times 10^{-15}\,\mathrm{cm}^2/\mathrm{s}$. This diffusion coefficient is about two orders of magnitude higher than that of atomic Si diffusion in GaAs, but it is in agreement with values found by Nutt *et al.* for Si-pair diffusion in highly δ-doped GaAs samples.[10] The fits together with experimental spectra are shown in Fig. 3. The slight broadening of the quasielastic peak is well reproduced. The measured spectrum for $E_0 = 15$ eV and $\theta = 70°$ is shown in greater detail in Fig. 6 together with the calcu-

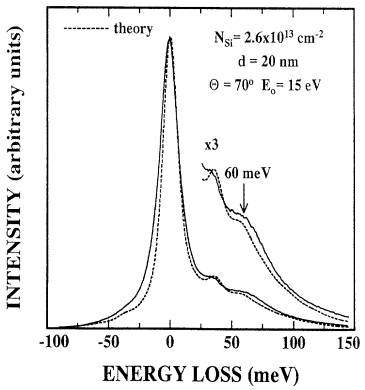

FIG. 6. HREEL spectrum of a δ-doped GaAs structure with $2.6\times10^{13}\,\mathrm{cm}^{-2}$ silicon atoms introduced 20 nm beneath the surface (solid line, magnified spectrum from Fig. 3). In the dashed line the simulated spectrum according to a simple doping profile model is given [see Fig. 4(b)]. The energy loss at 60 meV is caused by excitation of a plasmon mode in the quasi-2D electron gas of the δ layer.

lated one. The observed energy loss at 60 meV is in good agreement with the simulation from the doping model.

The integrated intensity of the broad loss continuum observed for the low-doped samples (Fig. 2) contains the sum of all elastically and inelastically scattered electrons accepted by the analyzer. If we approximately assign the offset in the linear dependence to the elastically scattered electrons, then the remaining amount of inelastically scattered electrons is proportional to the kinematic factor $1/k_0 \cos\theta$. The product $k_0 \cos\theta$ is proportional to the velocity component of the incident electrons normal to the surface and thus $1/k_0 \cos\theta$ is proportional to the time τ the incident electrons reside close to the GaAs surface. Therefore the loss probability of the electrons is proportional to τ, as expected for excitation of low-energy surface modes.[21]

The doping models described above yield good fits to our HREEL spectra and they seem to be appropriate pictures to describe the physical properties of our δ structures. It is, however, useful to reach a more detailed understanding of the physical origin of the observed characteristic spectral features. We will show now qualitatively that the broad loss continuum at low loss energies is caused only by confinement of the free-electron gas in a thin layer. For this purpose we make the simplifying assumption that the free-electron gas is embedded as an interlayer in a material without any other oscillators, in particular without any phonons. This quite simple three-layer model is shown in Fig. 7. A plasma layer of thickness d_2 is arranged between an oscillator-free top layer of thickness d_1 and an oscillator-free substrate. All layers in this model have the same high-frequency limit ϵ_∞ of the dielectric function. The plasma layer is described by a Drude oscillator. In the case of vanishing plasma damping the embedded free-electron plasma in the three-layer model has two collective surface modes $\omega_\pm$ for each wave vector k (see Appendix B).

The effect of confining the free electrons in a thin layer on the dispersion of both plasmon modes $\omega_\pm$ is explained in Fig. 8. We have chosen as an example material with the electronic properties of GaAs (but without any phonon oscillators), where the thickness of the top layer is d_1 =10 nm and the free-electron density of the confined plasma layer is $n = 10^{18}\,\mathrm{cm}^{-3}$. The dispersion $\omega_\pm(k)$ depends on the thickness d_2 of the free-electron layer. With decreasing d_2 the high-frequency mode ω_+ changes

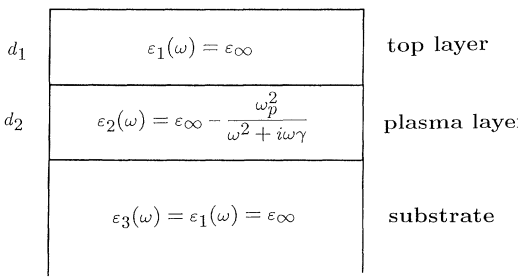

FIG. 7. Three-layer model with oscillator-free top layer, a confined free-electron layer, described by a Drude dielectric function, and an oscillator-free semi-infinite substrate.

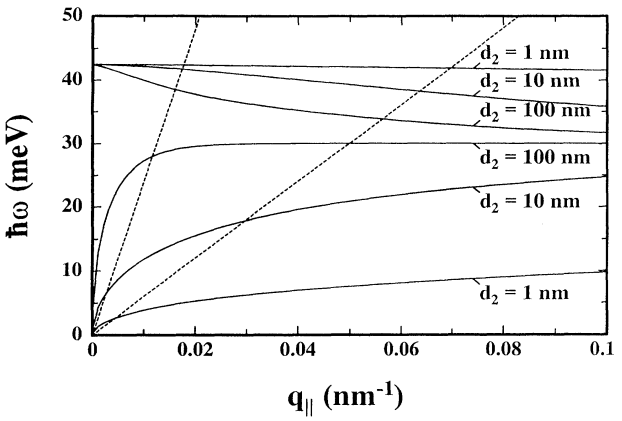

FIG. 8. Calculated dispersion relations $\omega(k)$ of the plasmon modes of the three-layer model of Fig. 7 for different thicknesses d_2 of the plasma layer (solid lines). The thickness of the top layer is $d_1 = 10\,nm$ and the volume density of the free-electron gas is $10^{18}\,\mathrm{cm}^{-3}$. The plasmon damping factor is neglected ($\gamma = 0$). The dashed lines indicate the range of the wave-vector transfer in a HREELS measurement.

only slightly. In contrast, the energy of the low-frequency mode ω_- decreases strongly with decreasing d_2. In the limit $d_2 \to 0$ this mode yields losses in the energy range close to the quasielastic peak where they cannot be resolved anymore by the HREEL spectrometer.

In HREELS measurements the component of the wave vector parallel to the surface is conserved in the scattering process, but there is no conservation rule for the perpendicular component of the wave vector.[21] Therefore the dispersion $\omega_\pm(k)$ is probed with wave-vector transfer $q_\parallel$ (parallel to the surface). For small-angle scattering $q_\parallel$ may be estimated to[21]

$$q_\parallel = \frac{k_0 \sin\theta}{2E_0}\,\hbar\omega. \tag{1}$$

From Eq. (1) it follows that the phase velocity $\omega(q_\parallel)/q_\parallel$ of the surface excitation is constant for given E_0 and θ in the experiment. The dashed lines in Fig. 8 indicate the limits of this experimental range for our HREEL spectrometer. Thereby the low-frequency mode ω_- is probed in an energy range close to the resolution of the HREEL spectrometer.

While Fig. 8 provides information about the energies of the plasmon modes in the model of a confined electron gas, we have to consider the intensity of these modes in a HREELS measurement. The structure of the loss intensities in a HREEL spectrum is dominated by the energy-loss function $\mathrm{Im}\{-1/[\tilde{\epsilon}(\omega, \mathbf{k}) + 1]\}$.[21] In order to calculate the energy-loss function for the three-layer model we reintroduce a finite plasmon damping $\gamma \neq 0$ into the plasma layer.

As an example the energy-loss function with $d_1 = d_2 =$ 10 nm, $E_0 = 2.5$ eV, and $\theta = 60°$ is shown in Fig. 9 for various free-electron densities. Both the high- and low-frequency modes shift to higher energies with increasing electron density. Notice the strong broadening of the low-

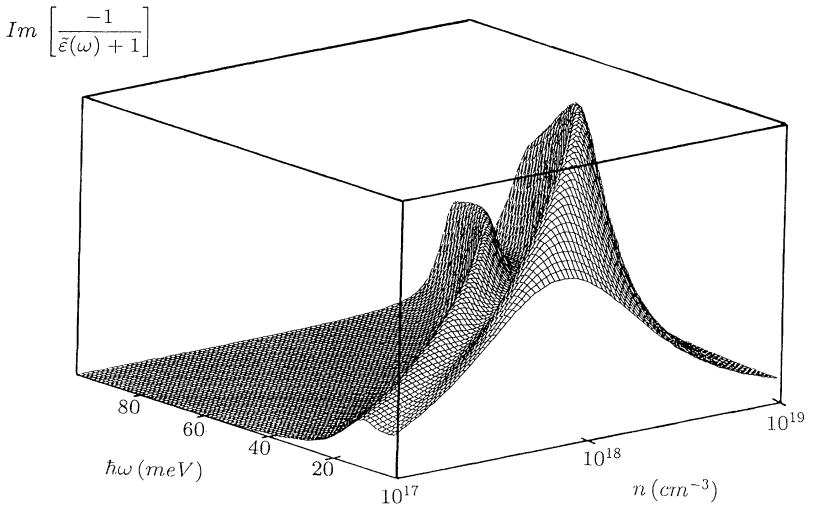

FIG. 9. Calculated surface energy-loss function of the three-layer model of Fig. 7 for a hypothetical material resembling GaAs in its electronic properties. The thicknesses of the top layer and the plasma layer are both 10 nm. The free-electron mobility is 1000 cm/V s and the kinetic energy of the primary electrons is $E_0 = 2.5$ eV with an incident angle $\theta = 60°$. The low- and high-frequency quasi-2D plasmon modes are shown for different volume densities n of the free electrons in the plasma layer.

frequency mode at smaller energies. These small energy losses cause the broadening of the quasielastic peak. The broadening strongly depends on the free-electron density in the plasma layer. There is a maximum intensity of small energy losses for an electron density of about 10^{18} cm^{-3} in this example. The plot represents the structure of the energy losses, but does not show the intensities in a HREELS measurement. We get an estimation of the HREELS intensities by multiplying the energy-loss function with $f(\omega)/\hbar\omega$, where $f(\omega) = [1-\exp(-\hbar\omega/k_BT)]^{-1}$. Therefore the higher-energy losses in Fig. 9 are supressed compared to the low-energy losses. An observation of the high-frequency mode becomes possible at higher primary energies, where the plasmon modes become sharper and the high intensity of low-energy losses is reduced (not shown here).

This example clearly shows that the confinement of free electrons in a thin layer leads to a high intensity for low-energy losses in a HREELS measurement. Therefore, the strong energetic broadening of the quasielastic peak as observed for the present low-doped δ structure can be interpreted in terms of the low-frequency mode of a quasi-2D plasmon. The high-frequency mode is not seen here. For the high-doped δ structure the broadening of the quasielastic peak is much smaller. The observed new loss feature at 60 meV (Fig. 6) is attributed to the high-frequency mode of the quasi-2D plasmon in the δ layer (Fig. 9). It must be emphasized that the present analytic treatment of the three-layer model can only qualitatively explain the observed loss spectra since phonon oscillators as in GaAs are not taken into account. For a quantitative description coupling of surface phonons to the plasmon modes cannot be neglected. However, this coupling is taken into account in the simulation of the HREEL spectra arising from the model of the dopant distribution.

V. CONCLUSION

In this paper we have shown that quasi-2D plasmon modes of a single δ-doped layer sufficiently close to the GaAs surface can be observed with high-resolution electron-energy-loss spectroscopy. The loss features in the HREEL spectra are attributed to low- and high-frequency collective surface modes of the confined free-electron gas in the δ-doped layer. A three-layer model is presented to understand the nature of these modes in relatively simple physical terms. The results are appropriately described by the classical dielectric scattering theory even for very thin layers with 2D quantization.

We have used the loss features of the quasi-2D plasmon modes in the HREEL spectra to develop a model of the spatial donor density profile of the δ-doped samples. In our model these profiles are rather simply described as one (low-doped samples) or two (high-doped samples) rectangular-shaped functions. However, simulations of the HREEL spectra according to this simple doping model produce good fits to the spectra measured on our samples. In the case of the low-doped sample all silicon atoms are electrically active and segregate into the direction of growth. For high-doping concentrations, an additional symmetric Si-pair diffusion with respect to their original location with a diffusion coefficient of $D = 2.8 \times 10^{-15}$ cm^2/s is found.

SIMS and CV profiling techniques are limited in their application when the δ doping is very close to the surface. Therefore HREELS may provide a new and potentially important method for studying the spatial donor profile of a δ-doped layer close to the surface.

ACKNOWLEDGMENTS

We would like to thank Ph. Lambin for providing the computer program to simulate HREEL spectra of an arbitrary multilayered target. We thank R. Kohleick for performing the UPS measurements.

APPENDIX A: SIMULATION OF HREEL SPECTRA

The density profile $n(z)$ of free electrons for the assumed doping profile (Fig. 4) has been calculated by

using the Hartree approximation. The Schrödinger and Poisson equations have been solved self-consistently. Band bending, segregation of the donors, and the nonparabolicity of the conduction band have been taken into account. Background doping of the GaAs of less than $10^{14}\,\mathrm{cm}^{-3}$ was neglected. The remaining free electrons of the δ layer are Fermi distributed among the 2D subbands and the sum of the squares of the electron wave functions of the subbands was used to derive the free-electron density profile $n(z)$. The calculated free-electron profile is then used as an input for a simulation of the HREEL spectra, as described below.

Since the HREEL spectrometer detects only small angle deviations from the specular direction, the incident electrons couple to exitations in the sample essentially via dipole scattering (dielectric theory). It is therefore appropriate to describe the sample in a macroscopic picture by an effective frequency-dependent dielectric function. The spatial free-electron density profile $n(z)$ has been approximated by a histogram n_j of about 20 layers to simulate the effective dielectric function. Each layer of thickness d_j in the histogram is described by the dielectric function

$$\epsilon_j(\omega) = \epsilon_\infty + \frac{(\epsilon_{\mathrm{st}} - \epsilon_\infty)\,\omega_{\mathrm{TO}}^2}{\omega_{\mathrm{TO}}^2 - \omega^2 - i\omega\Gamma} - \frac{\omega_{p,j}^2}{\omega^2 + i\omega\gamma}. \tag{A1}$$

Here ϵ_{st} and ϵ_∞ are the zero- and high-frequency limits of the dielectric function, ω_{TO} the transverse optical phonon frequency, and Γ the phonon damping factor. The values for the phonon part of the dielectric function are well known from the literature.[22] The free electrons are described by the Drude model with the plasma frequency $\omega_{p,j}$ of the jth layer and the plasmon damping factor γ. The plasma frequency is given by $\omega_{p,j}^2 = n_j e^2/m\epsilon_0$, with n_j the free-electron 3D density of the jth layer in the histogram, and m the mean effective mass of free electrons in the 2D subbands. The plasma damping is considered to be only Ohmic. Therefore we have estimated γ by the measured free-electron Hall mobility $\gamma = e/m\mu_{\mathrm{Hall}}$.

Lambin, Vigneron, and Lucas have derived the effective dielectric function $\tilde{\epsilon}(\omega, \mathbf{k})$ of a multilayered system by dielectric scattering theory.[23] The electrons are considered as classical particles, while the multiple absorption or emission of phonons or plasmons are described in a quantum-mechanical picture. From solving a Riccati differential equation they derived a continued fraction for $\tilde{\epsilon}(\omega, \mathbf{k})$, which may be rewritten to the recursive equation[23]

$$\tilde{\epsilon}(\omega, \mathbf{k}) = \tilde{\epsilon}_1 \tag{A2}$$

with

$$\tilde{\epsilon}_j = \epsilon_j \frac{\tilde{\epsilon}_{j+1} + \epsilon_j \tanh(kd_j)}{\epsilon_j + \tilde{\epsilon}_{j+1} \tanh(kd_j)}. \tag{A3}$$

Here ϵ_j is the dielectric function Eq. (A1) and d_j is the thickness of the jth layer. The first layer ($j = 1$) is close to the surface, the last layer ($j = b$) is the semi-infinite substrate, yielding $\tilde{\epsilon}_b = \epsilon_b$.

The simulation of HREEL spectra is based on an integration of the classical loss probability for an electron losing the energy $\hbar\omega$ within a range of surface wave vectors which scatter the probing electrons into the detector aperture. For the scattering cross section the standard dielectric formalism is applied.[21] The temperature of the samples (300 K) is taken into account by a Poisson distribution of multiple-loss peaks. Also, a convolution of the calculated losses with the transmission function of the HREEL spectrometer is performed. Details are given elsewhere.[23]

Several HREEL spectra have been simulated using the histogram profile n_j of the free electrons for different spreading lengths of the donors. In each layer the phonon oscillator and the plasmon Drude term of Eq. (A1) are used. Then the calculated HREEL spectra were compared to our experimental data. The doping profiles resulting as best fits to our HREEL data in the entire experimental range of E_0 and θ are shown in Fig. 4.

APPENDIX B: SURFACE MODES OF A CONFINED FREE-ELECTRON LAYER

Consider a three-layer system composed of a top layer of thickness d_1 with a dielectric function ϵ_1, an additional layer of finite thickness d_2 with another dielectric function ϵ_2, and a semi-infinite substrate, again with a dielectric function ϵ_1 as for the top layer. Then Eqs. (A2) and (A3) lead to an expression for the effective dielectric function $\tilde{\epsilon}_{3L}(\omega, \mathbf{k})$ of the three-layer system, given by

$$\tilde{\epsilon}_{3L}(\omega, \mathbf{k}) = \epsilon_1 \left[1 - \frac{2\,X_1\,(1 - X_2)}{X_1\,(1 - X_2) + \Delta(\omega)^{-1} - X_2\,\Delta(\omega)}\right], \tag{B1}$$

where we have used the notations

$$X_j = \exp(-2kd_j) \tag{B2}$$

and

$$\Delta(\omega) = \frac{\epsilon_1(\omega) - \epsilon_2(\omega)}{\epsilon_1(\omega) + \epsilon_2(\omega)}. \tag{B3}$$

The dispersion relations of the surface modes in this model are readily found by noting that they appear as poles of the energy-loss function $\mathrm{Im}\{-1/[\tilde{\epsilon}(\omega, \mathbf{k}) + 1]\}$. From Eq. (B1) the condition $\tilde{\epsilon}_{3L}(\omega, \mathbf{k}) + 1 = 0$ gives

$$\frac{\epsilon_1 + 1}{\epsilon_1 - 1}\left[\Delta(\omega)^{-1} - X_2\,\Delta(\omega)\right] = X_1\,(1 - X_2). \tag{B4}$$

In Eqs. (B1)–(B4) the dielectric function $\epsilon_1(\omega)$ of the top layer and the substrate, and the dielectric function $\epsilon_2(\omega)$ of the interlayer are still general. The surface modes of a confined free-electron layer are found by attributing ϵ_2 of the interlayer to the free-electron gas as shown in Fig. 7. For simplicity we neglect all phonon oscillators in this layered structure to derive solely the influence of a Drude electron gas located in the second layer. The top layer and the substrate are described by the dielectric constant

$$\epsilon_1(\omega) = \epsilon_\infty \tag{B5}$$

TABLE II. Limits of low- and high-frequency modes Eq. (B10) of a confined free-electron plasma (Fig. 7).

	$kd_2 \to 0$ (thin plasma layer)	$kd_2 \to \infty$ (thick plasma layer)
Independent of kd_1	$\omega_+ \to \frac{\omega_p}{\sqrt{\epsilon_\infty}}$ bulk frequency	$\omega_- \to \frac{\omega_p}{\sqrt{2\epsilon_\infty}}$ interface mode
$kd_1 \to 0$ (thin top layer)	$\omega_- \to \omega_p \sqrt{\frac{kd_2}{\epsilon_\infty+1}} \to 0$	$\omega_+ \to \frac{\omega_p}{\sqrt{\epsilon_\infty+1}}$ surface mode
$kd_1 \to \infty$ (thick top layer)	$\omega_- \to \omega_p \sqrt{\frac{kd_2}{2\epsilon_\infty}} \to 0$	$\omega_+ \to \frac{\omega_p}{\sqrt{2\epsilon_\infty}}$ interface mode

and the second layer of the three-layer model is considered as a plasma layer with the Drude dielectric function

$$\epsilon_2(\omega) = \epsilon_\infty - \frac{\omega_p^2}{\omega^2 + i\omega\gamma}. \tag{B6}$$

Inserting Eqs. (B5) and (B6) into Eq. (B4) and neglecting the plasmon damping factor ($\gamma = 0$) we are led to the secular equation

$$\omega^4 - \omega^2[(1+X_2)\,\omega_{\rm I}^2 + (1-X_2)\,\omega_{SD}^2] + (1-X_2)\,\omega_{\rm I}^2\omega_{SD}^2 = 0, \tag{B7}$$

where

$$\omega_{\rm I}^2 = \frac{\omega_p^2}{2\epsilon_\infty} \tag{B8}$$

is the interface mode between two semi-infinite media described by the dielectric functions $\epsilon_1(\omega)$ of Eq. (B5) and $\epsilon_2(\omega)$ of Eq. (B6), respectively, and

$$\omega_{SD}^2 = \frac{\omega_p^2}{2\epsilon_\infty}\left[1 + X_1\,\frac{\epsilon_\infty - 1}{\epsilon_\infty + 1}\right] \tag{B9}$$

is the dispersion relation of a surface plasmon of a homogenously doped sample, described as a semi-infinite free-electron layer with the Drude dielectric function $\epsilon_2(\omega)$ and an oscillator-free depletion layer of thickness d_1 above. The solutions of Eq. (B7) may be written as

$$\omega_\pm^2 = \frac{\omega_p^2}{2\epsilon_\infty}\left[1 + C \pm \sqrt{X_2 + C^2}\right] \tag{B10}$$

with the abbreviation

$$C = \frac{1}{2}\,\frac{\epsilon_\infty - 1}{\epsilon_\infty + 1}\,X_1\,(1 - X_2). \tag{B11}$$

In order to show the behavior of Eq. (B10), the limits of low- and high-frequency modes $\omega_\pm$ for very thin and very thick layers are compared in Table II.

[1] K. Ploog, M. Hauser, and A. Fischer, Appl. Phys. A **45**, 233 (1988).

[2] F. Koch, *Interface, Quantum Wells and Superlattices*, Vol. 179 of *NATO Advanced Study Institute, Series B: Physics*, edited by C. R. Leavens and R. Taylor (Plenum, New York, 1988).

[3] F. Koch, A. Zrenner, and M. Zachau, *Proceedings of the International Winter School, Mauterndorf, Austria, 1986*, Vol. 67 of Solid-State Sciences, edited by G. Bauer, F. Kuchar, and H. Heinrich (Springer-Verlag, Berlin, 1986).

[4] A. Zrenner, F. Koch, and K. Ploog, in *Gallium Arsenide and Related Compounds*, Proceedings of the 14th International Symposium on GaAs and Related Compounds, Heraklion, Greece, 1987, edited by A. Cristou and H. S. Rupprecht, IOP Conf. Proc. No. 91 (Institute of Physics, Bristol, 1988).

[5] A. Zrenner, F. Koch, and K. Ploog, Surf. Sci. **196**, 671 (1988).

[6] E.F. Schubert, H.S. Luftman, R.F. Kopf, R.L. Headrick, and J.M. Kuo, Appl. Phys. Lett. **57**, 1799 (1990).

[7] Ph. Jansen, M. Meuris, M. Van Rossum, and G. Borghs, J. Appl. Phys. **68**, 3766 (1990).

[8] A-M. Lanzillotto, M. Santos, and M. Shayegan, J. Vac. Sci. Technol. A **8**, 2009 (1990).

[9] M. Santos, T. Sajoto, A.-M. Lanzillotto, A. Zrenner, and M. Shayegan, Surf. Sci. **228**, 255 (1990).

[10] H.C. Nutt, R.S. Smith, M. Towers, P.K. Rees, and D.J. James, J. Appl. Phys. **70**, 821 (1991).

[11] A. Zrenner, Appl. Phys. Lett. **55**, 156 (1989).

[12] E.F. Schubert, R.F. Kopf, J.M. Kuo, H.S. Luftman, and P.A. Garbinski, Appl. Phys. Lett. **57**, 497 (1990).

[13] H.K. Kim, T.E. Schlesinger, and A.G. Milnes, J. Electron. Mater. **19**, 139 (1990).

[14] J. Wagner, M. Ramsteiner, W. Stolz, M. Hauser, and K. Ploog, Appl. Phys. Lett. **55**, 978 (1989).

[15] M. Santos, T. Sajoto, A. Zrenner, and M. Shayegan, Appl. Phys. Lett. **53**, 2504 (1988).

[16] J. Wagner, M. Ramsteiner, W. Stolz, M. Hauser, and K. Ploog, in *Gallium Arsenide and Related Compounds*, Proceedings of the 16th International Symposium on GaAs and Related Compounds, Karuizawa, Japan, 1989, edited by T. Ikoma and H. Watanaba, IOP Conf. Proc. No. 106 (Institute of Physics, Bristol, 1990).

[17] S.P. Svensson, J. Kanski, T.G. Andersson, and P.-O. Nilsson, J. Vac. Sci. Technol. B **2**, 235 (1984).

[18] R.B. Beal, J.B. Clegg, and J.J. Harris, Semicond. Sci. Technol. **3**, 612 (1988).

[19] A. Zrenner, F. Koch, R.L. Williams, R.A. Stradling, K. Ploog, and G. Weimann, Semicond. Sci. Technol. **3**, 1203 (1988).

[20] E.F. Schubert, J.M. Kuo, R.F. Kopf, A.S. Jordan, H.S. Luftman, and A.S. Hopkins, Phys. Rev. B **42**, 1364 (1990).

[21] H. Ibach and D.L. Mills, *Electron Energy Loss Spectroscopy and Surface Vibrations* (Academic, New York, 1982).

[22] A.H. Kachare, W.G. Spitzer, F.K. Euler, and A. Kahan, J. Appl. Phys. **45**, 2938 (1974).

[23] Ph. Lambin, J.P. Vigneron, and A.A. Lucas, Phys. Rev. B